

Formation of terraced, nearly flat, hydrogen-terminated, (100) Si surfaces after high-temperature treatment in H₂ of single-crystalline silicon

G. F. Cerofolini*

STMicroelectronics, 20041 Agrate, Milan, Italy

C. Galati, S. Reina, L. Renna, and N. Spinella

STMicroelectronics, Stradale Primosole 50, 95121 Catania, Italy

D. Jones and V. Palermo

ISOF-CNR, Via Gobetti 101, 40129 Bologna, Italy

(Received 25 May 2005; revised manuscript received 19 July 2005; published 26 September 2005)

Among the processes devoted to the preparation of chemically homogeneous (100) silicon surfaces, the ones for hydrogen termination are the most promising, especially in view of the remarkable environmental stability of such surfaces. The simplest way to produce hydrogen-terminated silicon (attack of a sacrificial, thermally grown, oxide in aqueous solution of HF) results in rough, strongly heterogeneous (although with prevailing dihydride terminations) surfaces. These surfaces can, however, be flattened and homogenized by treating them in H₂ at high temperature (>850 °C). The morphological and chemical changes undergone by the surface during the treatment are studied *ex situ* (via x-ray-photoelectron spectroscopy, atomic force microscopy, scanning tunneling microscopy, infrared absorption spectroscopy in the attenuated total reflection mode, reflection high-energy electron diffraction, and thermal programmed desorption) and the mechanisms responsible for them are discussed.

DOI: [10.1103/PhysRevB.72.125431](https://doi.org/10.1103/PhysRevB.72.125431)

PACS number(s): 68.43.Mn, 34.50.Dy, 82.30.Hk

I. INTRODUCTION

The (100) surface of silicon (the one with the widest range of applications in integrated-circuit processing) is not a cleavage surface, and is typically obtained by cutting single crystals along planes as close as possible to (100) and chemomechanically polishing the resulting rough surface with colloidal SiO₂ dispersed in KOH aqueous solution.^{1,2} As a consequence, the actual (local) orientation resulting after cutting and polishing is controlled by the alignment uncertainties of the sawing and lapping machines and by the roughness related to the etching and polishing processes. The final result is a misoriented surface, with a local peak-to-valley roughness on the nanometer length scale.

The polishing procedure, moreover, produces surfaces with prevailing hydrogen terminations,^{3,4} but containing residual oxocenters (Si-O-Si and Si-O-H), too. A lot of work has been carried out to prepare chemically homogeneous and environmentally stable surfaces. The oxoterminated surfaces are not suitable for that goal because of two reasons: (i) the early stages of oxidation produce a chemically heterogeneous zone⁵ where the silicon oxidation state is distributed between 0 and 4; and (ii) exposed to humid air at room temperature, surfaces containing oxocenters undergo further oxidation.^{6,7}

The common belief that hydrogen-terminated silicon would be indefinitely stable (on the laboratory time scale) in air at room temperature, explains why several methods have been developed for the hydrogen passivation of (100) silicon, including:

(1) Chemical attack with an aqueous solution of HF (HF_{aq}) of a sacrificial, thermally grown, oxide.

(2) Demolition of such hydrogen terminations by heat treatment at moderate temperature (say, $T \leq 550$ °C) (Ref. 8) followed by the exposure of the resulting clean 2×1 -reconstructed surface to a few langmuirs of atomic hydrogen H (in turn obtained by the dissociation of H₂ after contact with a hot tungsten filament).

(3) Exposure of the HF_{aq}-prepared surface to H₂ at sub-atmospheric pressure (typically in the interval 10^2 – 10^3 Pa) and moderate temperature (typically around 800 °C).

Hydrogen-terminated surfaces can greatly differ according to their preparation:

(i) Process (1) results in 1×1 surfaces with a heterogeneous distribution of SiH₃, SiH₂, (prevalently) and SiH terminations.^{8,9}

(ii) Process (2) produces different reconstructions according to the temperature:¹⁰ (1) The 1×1 dihydride phase at 300 K; (2) 1.33 H monolayers with 3×1 reconstruction at 400 K; or (3) the monohydride phase with 2×1 reconstruction at 600 K (these are shown schematically in Fig. 1); and

(iii) Process (3) is invariably reported to result in 2×1 (100) SiH—the 2×1 reconstructed, monohydrogen terminated, (100) silicon surface.^{11–14}

We have, however, recently reported^{15–18} that the surface of commercial (100) Si wafers, after etching in HF_{aq}, baking in H₂ at subatmospheric pressure and high temperature (850–1100 °C), cooling to 670–700 °C in the same ambient, quenching to room temperature in N₂, and eventual exposure to air is terraced, nearly flat, highly homogeneous, 1×1 (re)constructed with dihydride terminations. This surface is referred to as 1×1 (100) SiH₂.

X-ray-photoelectron spectroscopy (XPS), atomic force microscopy (AFM), infrared absorption spectroscopy in the

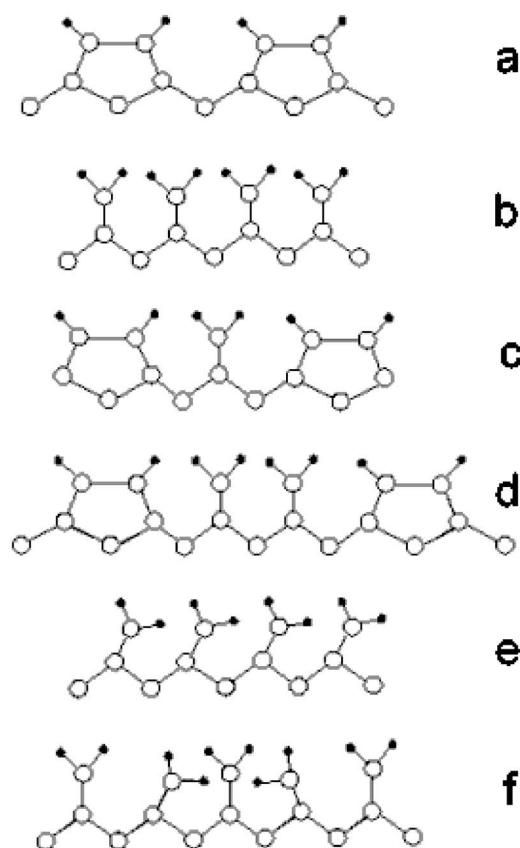


FIG. 1. Schematic of various hydrides occurring at the (100) silicon surface: (a) 2×1 monohydrides, (b) “classic” 1×1 dihydrides, (c) 3×1 alternating di- and mono-hydrides, (d) “split dimer” dihydrides between monohydride domains, (e) canted 1×1 dihydrides, (f) domain-boundary situation where dihydrides with elongated Si-Si backbonds alternate with canted dihydrides (see Ref. 35).

attenuated total reflection mode (ATR-IRAS), reflection high energy electron diffraction (RHEED), and thermal programmed desorption (TPD) were used to characterize these surfaces and understand the phenomena producing them.^{15–18} In this work we extend the experimental bases of our study providing atomic-scale information on the surface via scanning tunneling microscopy (STM).

II. EXPERIMENT

A. Preparation

The samples considered in this work were prepared in one of the following ways:

- Etching the as-received slice in HF_{aq} .
- Treating the HF_{aq} -etched surface in H_2 at moderate temperature (800–850 °C).
- Treating the HF_{aq} -etched surface in H_2 at high temperature (1100 °C).
- Oxidizing the surface treated in H_2 at 1100 °C with a $\text{H}_2\text{O}_2 + \text{H}_2\text{SO}_4$ (“piranha”) solution and removing the oxide formed with HF_{aq} .

Samples (a) were prepared via standard cleaning, etching in diluted HF_{aq} , and rinsing in deionized O_2 -free water,

single crystalline, Czochralski grown, (100) oriented, *p* type, boron doped, silicon slices with resistivity 1.5–5 Ω cm.

The etched samples were mounted in a commercially available load-locked single-wafer lamp-heated reactor (AMAT Centura) where they were

- *Baked* in H_2 at a pressure of 1.1×10^4 Pa in an open reactor (the hydrogen flux being of 2.2×10^{-2} mol s^{-1}) at 850 °C for 1 or 3 min [samples (b₁) or (b₃), respectively] or at 1100 °C for 3 min [samples (c)];

- *Cooled* in the same environment to 670–700 °C at a rate of about -10 °C s^{-1} ;

- *Quenched* to room temperature at an uncontrolled rate (of the order -10^2 °C s^{-1}) after moving them into a sample transfer chamber in an N_2 atmosphere at a pressure of 1.1×10^4 Pa (quenching being allowed by the relatively high N_2 pressure).

Additional samples, referred to as (b’), were also prepared from the HF_{aq} -etched wafer by baking in H_2 at 800 °C for 20 min; cooling to 300 °C in the same environment; and quenching to room temperature in N_2 .

The main interest here is for samples (c); samples (b₁) and (b₃) are considered because they are putatively able to “photograph” intermediate situations of the evolution from (a) to (c); sample (b’) is considered because its preparation conditions border upon (while not overlapping) those considered in Refs. 11 and 12; the reason for sample (d) will be clarified later.

The use of nitrogen in the quenching stage requires some comments. In fact, a flowing gas at relatively high pressure is required to quench the situation resulting after the cooling stage. Since the use of H_2 is prohibited for safety reason, N_2 was chosen on the basis of its inertness toward silicon at $T < 700$ °C. The correctness of this assumption was checked by verifying that the nitrogen amount at the silicon surface (measured through the intensity of the N 1s signal) was below the detection limit (say, 0.1% at.). A weak surface nitridation was only observed in side experiments¹⁹ after an exposure to N_2 at 850 °C.

Another point of some importance concerns the possible traces of contaminants (like H_2O) contained in the H_2 . In fact, the low sticking coefficient of H_2 compared with that of, for instance, H_2O magnifies the effective concentration of the latter by many orders of magnitude. It is however observed that in our experiments the surface did not manifest any evidence for oxidized silicon (as demonstrated by the Si 2p spectra of Fig. 2, shown later), in agreement with similar experiments carried out in other laboratories at subatmospheric H_2 pressure.^{11,12} Of course *catalytic* effects due to oxygen cannot be ruled out, but such effects should also occur in experiments in a UHV, due to the oxygen amount contained within a diffusion length from the silicon surface (the concentration of interstitial oxygen in Czochralski silicon being of the order of 4×10^{17} cm^{-3}).

B. Analysis

After storing in air at room temperature for a few hours, the samples underwent an *ex situ* experimental characterization using the following techniques: XPS, AFM, STM, ATR-IRAS, RHEED, and TPD.

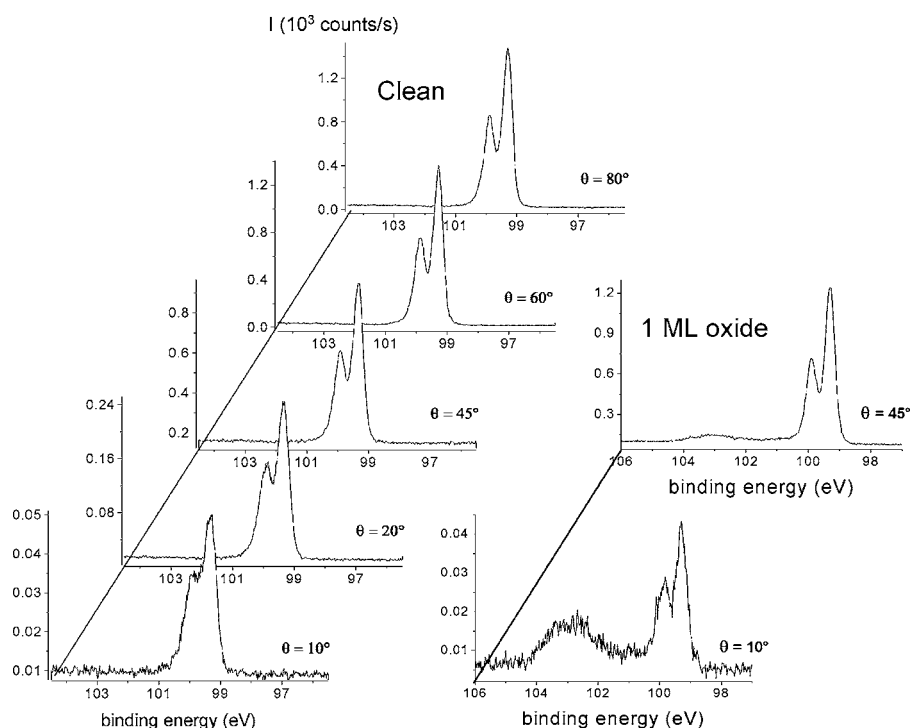


FIG. 2. Si 2p spectra taken at five different take-off angles of (100) silicon baked at 1100 °C following exposure to air at room temperature for several hours (left) or from a (100) silicon surface covered with a grown SiO₂ film of approximately one monolayer (right). The intensity scales were adjusted to have all maxima the same height.

The XPS spectra were detected mounting the samples in a PHI ESCA/SAM 5600 Multitechnique spectrometer with monochromatized x-ray beam.²⁰ The AFM measurements were carried out in the tapping mode with either a Digital Instruments Multimode apparatus¹⁵ or an NT-MTD instrument.¹⁸ The STM measurements were carried out in a UHV Omicron system using +1 V sample bias. The IRAS measurements were carried out using a Harrick GATR germanium single reflection ATR accessory.¹⁸ The TPD measurements were carried with a DCA-600 molecular-beam-epitaxy apparatus.¹⁵ The evolution of the silicon surface structure during heating in an ultrahigh vacuum (UHV) was determined via RHEED using a SteiB apparatus.¹⁵

III. RESULTS

It is anticipated that except for the terrace step length (discussed in Sec. III B and anyway controlled by the cutting conditions), the characteristics of different samples prepared with any given method were found to be remarkably similar, so that the data presented in the following may be considered representative of the preparation procedure.

A. X-ray photoelectron spectroscopy

The XPS spectra of a typical sample (c) are shown in the left-hand side of Fig. 2 for five takeoff angles. For comparison purposes, equivalent spectra from a surface covered by approximately one monolayer of oxidized silicon (with binding energy centered on ≈ 103 eV) (Ref. 5) are shown in the right-hand side of the figure. The comparison shows that even for the lowest takeoff angle, sample (c) does not show any evidence (within the XPS sensitivity limits) for oxidized silicon.¹⁶

B. Atomic force microscopy

The AFM micrographs of the surfaces of samples (a), (b₃), (c), and (d) are summarized in Fig. 3. The comparison shows that the annealing in H₂ flattens the surface and eventually produces a terraced surface.

Figure 4, showing the AFM micrographs of the surfaces of samples (a), (b₁), and (b₃) demonstrates that the temperature which allows a rough-to-flat transformation (at least on the laboratory time scale) is in the interval 800–850 °C, this transformation being completed at 850 °C in a few minutes.

The steps forming the terrace of sample (c) are separated either by nearly straight edges or by very irregular edges, alternatively. This structure is typically observed²¹ for clean 2×1 (100) surfaces, with step heights of just 0.136 nm. The terraces are not atomically flat, but rather contain several small domains: The ones shown as bright spots are mesas, while the ones shown as dark spots are hollows; mesas and hollows are separated from the embedding terrace by a distance of just one atomic step.

Table I shows that the morphological changes following transitions (a) \rightarrow (b₁) \rightarrow (b₃) \rightarrow (c) are associated with a roughness reduction, measured by the standard deviation of the surface profile from the average plane.

C. Scanning tunneling microscopy

In general, the HF_{aq} attack of (100) Si results in “fuzzy” images. Even though under special pH conditions the HF_{aq} etching results in surfaces with nearly atomic resolution (giving evidence for 1×1 symmetry^{22,23}), the STM analysis of HF_{aq}-etched samples (a) followed by atmospheric exposure did not provide any evidence for regularity.²⁴ Images with atomic resolution were, however, obtained for samples (c) following transport and insertion into the UHV system even

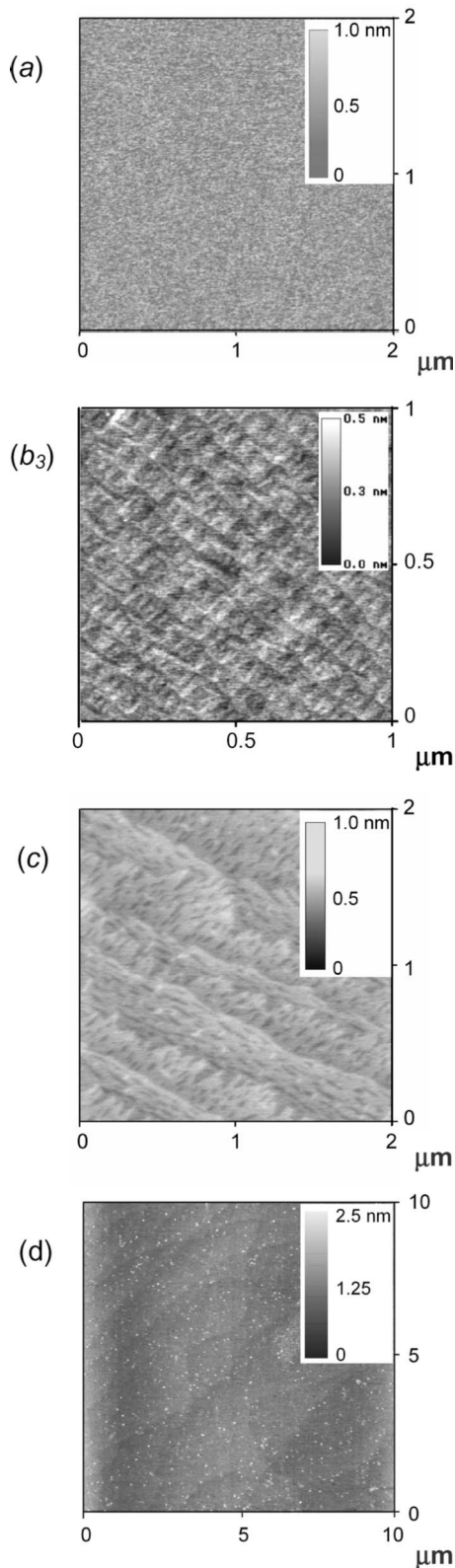


FIG. 3. Comparison of atomic-force micrographs of (100)-Si surfaces resulting after: (a) etching in HF_{aq} an as-received slice; (b₃) treating the HF_{aq} -etched surface in H_2 at 850 °C for 3 min; (c) treating the HF_{aq} -etched surface in H_2 at 1100 °C for 3 min; and (d) oxidizing the sample baked in H_2 at 1100 °C with a $\text{H}_2\text{O}_2 + \text{H}_2\text{SO}_4$ (piranha) solution and etching the resulting oxide in HF_{aq} .

without further treatment. However, the time necessary, following treatment of the sample, for its removal from the hydrogenation chamber, packaging, and transportation to the STM instrument significantly affected the sample surface and thus the STM images obtained. The images in Fig. 5 show graphically the nature of such changes over a relatively large area for samples whose exposure to air was different by a factor of about 2, on the time scale of $10\text{--}10^2$ h.

The figure shows small (1–5 nm in diameter) darker zones, interpreted as “holes” (or “pits”) 0.2–1.0 nm deep, together with small bright zones of similar lateral dimensions, interpreted as “protrusions” with relative heights of 0.4–0.8 nm. These features are irregularly distributed over all areas of the samples. Although the changes were not systematically followed over time, a general increase in the number of darker features with a corresponding decrease in the brighter ones was observed on going from the fresher samples to the older ones.

Given the much higher quality of the STM images from the fresh samples, where the bright spots still predominate over the darker features, the more detailed discussion below of the higher resolution STM data will focus upon the results from these samples. This will also ensure greater validity when comparing the STM results with those from the other techniques obtained after similarly brief periods following hydrogenation. Although the surface structures observed did not change significantly, the clarity of the images improved after sample heating at ≈ 100 °C in the STM UHV system.

At a more detailed level, the STM measurements provided images with atomic resolution generally attributed to the 1×1 dihydride surface [see, for example, Fig. 6(b)].

The STM images also show the presence of 2×1 -like ordered structures [see Fig. 6(a)] which are different from the classical 1×1 dihydride structure shown in Fig. 6(b). The average profiles along the rows of atoms (compared in the lower part of the figure) both show exactly the same, characteristic surface silicon interatomic distance of approximately 4 Å, but with alternating intensities (corresponding to changes in tip-to-sample distance) in the case of the “ribbed” 2×1 structure shown in Fig. 6(a). Thus, these 2×1 structures correspond neither to the 2×1 monohydride [shown schematically in Fig. 1(a)] nor to the alternating 3×1 structure²⁵ [Fig. 1(c)] nor even to the much more stable, novel dihydride species known as “split dimers” observed on the 2×1 (100) SiH surface²⁶ [Fig. 1(d)] whose filled-state STM images show a dark center and lighter sides.

TABLE I. Standard deviation of the actual surface profile from the average plane in differently treated samples.

Sample	Morphology	Standard deviation (nm)
(a)	Rough	0.18
(b')	Rough	0.12
(b ₁)	Stepped	0.10
(b ₃)	Stepped	0.08
(c)	Stepped	0.05
(d)	Stepped	0.20

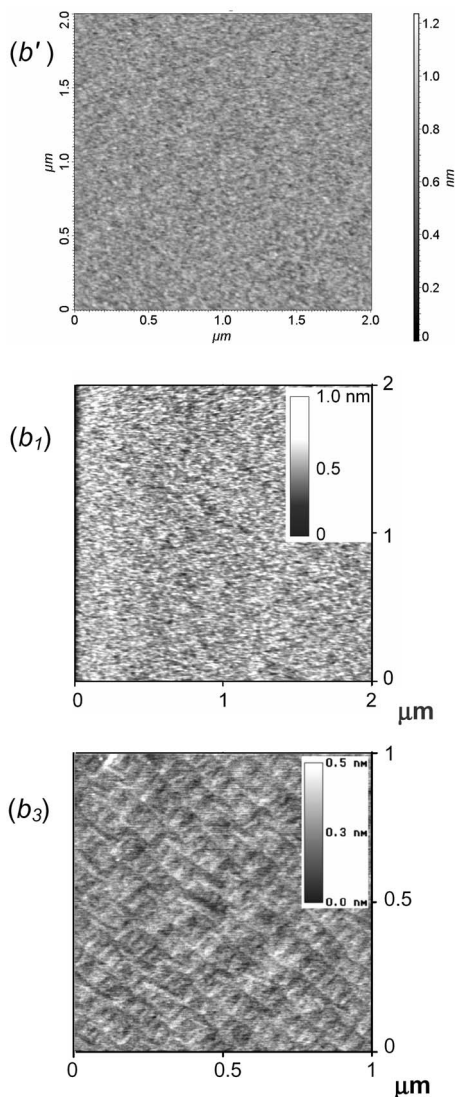


FIG. 4. Comparison of atomic-force micrographs of (100)-Si surfaces resulting after treating the HF_{aq} -etched surface in H_2 at (b') 800 °C for 20 min, (b₁) 850 °C for 1 min, or (b₃) 850 °C for 3 min.

D. Infrared absorption spectroscopy

The region of interest for Si-H vibrations lies in the interval 2000–2200 cm^{-1} . The ATR-IRAS spectra in that region for samples (a), (b'), (b₁), (c), and (d) are shown in Fig. 7. The spectrum of sample (a) shows a broad absorption band. The spectra of samples (b'), (b₁), and (c) are instead dominated by an intense sharp peak centered on a wave number of $(2100 \pm 1) \text{ cm}^{-1}$. The spectrum from sample (d) shows that the sequence of piranha oxidation and HF_{aq} etching restores the original heterogeneous distribution of Si-H bonds (however without modifying the preexisting surface topography, as demonstrated by the AFM evidence).

E. Thermal programmed desorption

The TPD spectra from samples (a), (b₁), and (c) are shown in Fig. 8. All of them give evidence for emission

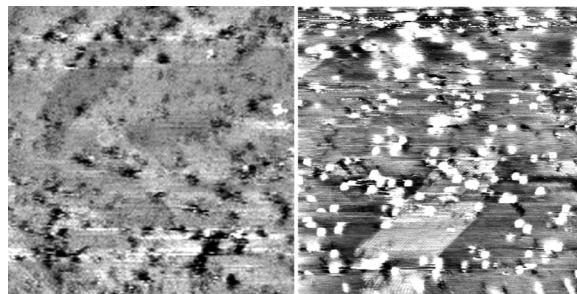


FIG. 5. Different large-scale characteristics in STM images ($100 \times 100 \text{ nm}^2$, +1 V sample bias, 0.09 nA tunneling current) of samples after $\approx 72 \text{ h}$ before insertion into the UHV system (left) and after $\approx 36 \text{ h}$ (right).

peaks at 300–350 °C and at $\approx 500 \text{ °C}$ (referred to as β_2 and β_1 , respectively¹⁰). Sample (c) gives also evidence for an emission peak (referred to as α) at $\approx 700 \text{ °C}$.

F. Reflection high-energy electron diffraction

The crystallographic evolution of the surface during TPD was followed by detecting the RHEED diffraction pattern. The diffraction pattern before heating was in all cases found to be the one characteristic of the 1×1 (100) surface. It evolved to that characteristic of the 2×1 (100) surface only at temperatures around 750 °C.

IV. DISCUSSION

The entire set of experimental data admits the following minimal interpretation: *The heat treatment in H_2 at T above 850 °C flattens the surface and eventually results in energetically homogeneous, hydrogen-terminated surfaces, and the surfaces so produced survive the cooling and quenching phases.*

In fact, although XPS is insensitive to hydrogen, the XPS data show that the surface does not undergo oxidation after exposure to air²⁷ and thus suggest that the hydrogen terminations certainly produced by the exposure to H_2 at high temperature survive the quenching stage and protect the surface against oxidation in air at room temperature for a duration on the time scale of 10^5 s .

The AFM data clearly show that the annealing in H_2 is responsible for a progressive flattening of the surface. This result extends previous observations¹² toward higher temperatures. In the samples baked at 1100 °C mesas and hollows are observable. Both are rotated by 90° with respect to adjacent atomic layers. The STM analysis confirms the structure resulting from AFM, showing that the hollows are etched areas in a single-layer terrace while the mesas are one-atomic-layer islands. This structure is typically observed for surfaces prepared under etching conditions,²¹ thus suggesting that the regular morphology of hollows and mesas is related to the flattening mechanism rather than to erratic factors (such as contamination, adsorption of foreign species, etc.). Remarkably enough, mesas and hollows are observed only in samples baked at 1100 °C (temperature at which the surface undergoes etching¹²) while are not observed at

850 °C (temperature at which the etching rate is negligible^{12,15}).

The heat treatments (even those at 800 °C for 20 min or at 850 °C for 1 min) produce the almost complete transformation of the original heterogeneous distribution of SiH_n ($n=1,2,3$) terminations into a homogeneous distribution. The heterogeneous nature of sample (a) is demonstrated by its broad absorption spectrum, covering the lines attributed to SiH_3 (at 2137 cm^{-1}), SiH_2 (at 2111 cm^{-1}), and SiH (at 2077 cm^{-1}) (the assignment is taken from Refs. 28 and 29). The homogeneous nature of surface terminations in the samples treated in H_2 is shown by their sharp absorption peaks, with a full width at half maximum of 11 cm^{-1} in (b₁) and of 7 cm^{-1} in (c). The comparison of spectra (c) and (d) shows that the final HF_{aq} etching results in a heterogeneous distribution of terminations. Since the sequence of piranha oxidation and HF_{aq} etching preserved the pre-existing terrace structure, the nearly homogeneous termination is intrinsically associated with the process in H_2 .

While the ATR-IRAS data provide unambiguous information on surface homogeneity, they however are by themselves unable to assess the nature (dihydride versus monohydride) of the chemical terminations. In fact, the silicon monohydride dimer $(\text{SiH})_2$ is characterized by symmetric (S) and antisymmetric (AS) stretching modes at 2099 and 2088 cm^{-1} , respectively,¹¹ while the silicon dihydride monomer SiH_2 has S and AS stretching modes at 2091 and 2104 cm^{-1} , respectively.³⁰ Thus the observed line at 2100 cm^{-1} might be attributed either to the S stretching mode of $(\text{SiH})_2$ or to the AS stretching mode of SiH_2 (a combination just in 1:1 proportion of them seems difficult to sustain). Since the sign of the S-AS splitting of SiH_2 is opposite to that of $(\text{SiH})_2$, the mode assignment is in principle possible via a comparison of the p -polarized with s -polarized IRAS spectra. However, the relative S/AS intensity depends so strongly on factors like environmental hydrocarbon contamination, surface roughness, etc.,¹¹ to make difficult this assignment. We have thus preferred to extract information on surface phase from RHEED and TPD—RHEED is indeed sensitive to surface reconstruction, while TPD is sensitive to surface composition.

As mentioned in Sec. III F, for all samples analyzed in this work the diffraction pattern before heating was found to be the one characteristic of the 1×1 (100) surface. The diffraction pattern evolved to be characteristic of the 2×1 phase only at temperatures of about 750 °C , in agreement with what is observed for the 1×1 (100) SiH_2 surface.³¹

For patchwise surfaces H_2 may be assumed to be desorbed from hydrogen-terminated silicon via the consecutive reactions sketched in Fig. 9. The β_1 peak is originated by H_2 elimination from $(\text{SiH})_2$ dimers while the β_2 peak is originated by H_2 elimination from vicinal SiH_2 groups, the migration energy of SiH_2 not being a limiting factor to this process.³² For the ideal phases 2×1 $(\text{SiH})_2$, 3×1 $(\text{SiH})_2$ - SiH_2 , and 1×1 SiH_2 the β_2 -to- β_1 intensity ratio I_{β_2}/I_{β_1} is therefore given by Table II.

The accurate determination of ratio I_{β_2}/I_{β_1} requires a quantitative description of the desorption kinetics (planned for another work). Qualitative estimates can however be rea-

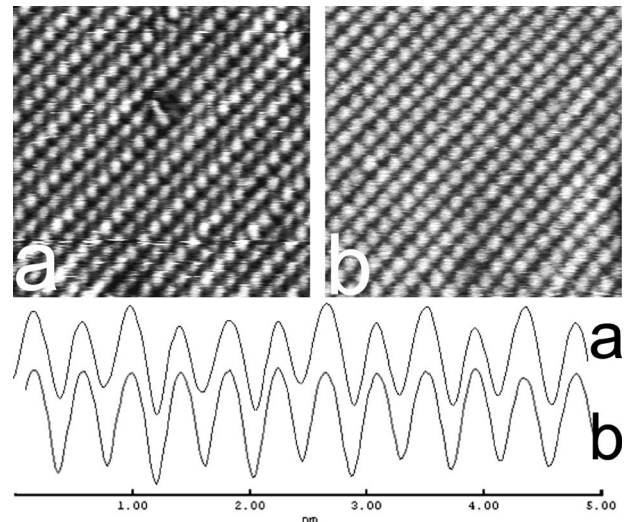


FIG. 6. STM images showing apparent changes in structure of the 1×1 (100) SiH_2 with changes in tip-sample distance: (a) 2×1 (100) SiH_2 with alternate rows (see also Ref. 36); (b) classical 1×1 . The lower part of the figure shows the differences between their respective average z profiles across the rows of atoms (see text). [Dimensions: (a) and (b) $7 \times 7\text{ nm}^2$. All images obtained with $+1\text{ V}$ sample bias and 0.08 nA tunneling current.]

sonably inferred and their comparison with the expected values given in Table II indicate that samples (b₁) and (c) have SiH_2 terminations.

In this scheme it seems somewhat disturbing that for sample (a) I_{β_2}/I_{β_1} is larger than 1. It is however noted that for rough and heterogeneous surfaces H_2 may also be desorbed via H_2 elimination from a vicinal pair of isolated SiH_2 and SiH . Since this process does not result in monohydride dimers $(\text{SiH})_2$, it cannot contribute to the β_1 peak and thus may be responsible for the occurrence $I_{\beta_2} > I_{\beta_1}$.

Roughness has contributions at several wavelengths: In the considered example, roughness may be thought of as having a contribution at long wavelengths (manifested as “morphology” in the terrace structure) and at short wavelength (“local roughness,” measured by the root mean square of the peak-to-valley distance). The experiment [showing that the sequence of piranha oxidation and HF_{aq} etching does not modify appreciably the terrace morphology whereas the local roughness increases (from 0.05 nm to about 0.2 nm) and so does the chemical heterogeneity (from a very sharp peak to a broadly distributed band)] suggests that *energetics and geometry are correlated only at short wavelengths*.

The total area explored by STM is too low to be representative of the whole silicon surface as probed by ATR-IRAS or XPS. Nonetheless, the explored surface of sample

TABLE II. β_2 -to- β_1 intensity ratio for the considered phases.

Phase	I_{β_2}/I_{β_1}
Ideal 2×1 $(\text{SiH})_2$	0
Ideal 3×1 $(\text{SiH})_2$ - SiH_2	1/3
Ideal 1×1 SiH_2	1

(c) was remarkably homogeneous and consistent with its ATR-IRAS spectrum shown in Fig. 7. Assuming that the prevailing structure detected by STM is the same as that responsible for the ATR-IRAS peak, STM identifies it as the dihydride surface on the basis of the “interatomic” distances. Figure 6 shows the presence of 1×1 and 2×1 symmetry in the STM images but both with the same interatomic distances as shown in the traces beneath the images. This 2×1 symmetry cannot correspond to the monohydride because the latter shows alternating interatomic distances due to the presence of the Si-Si dimer bond in the monohydride.

Calculations have shown^{33,34} that a canted structure [in Fig. 1(e)] is energetically advantageous for the 1×1 dihydride. The distortion in the dihydride canted phase reduces the repulsion between the hydrogens while weakening the Si-Si backbonds. Longer-range calculations³⁵ also showed the possibility of oppositely canted domains with the dihydride at the domain boundary having an elongated Si-Si backbond. If this were the case, the elongated bond might thus render the SiH_2 surface groups distinguishable in STM images. One possible hypothesis is that the structure observed here consists of alternating rows of canted-elongated-canted SiH_2 groups [Fig. 1(f)].

However, similar 2×1 structures on dihydride-terminated (100) Si surfaces, believed to be peculiar to the noncontact atomic force microscopy (NC-AFM) technique, were interpreted as being due to the attractive force of the AFM tip followed by self-organization of the dihydride rows.³⁶ The variations observed in those NC-AFM images on varying the tip-sample distance are similar to those observed in our images as shown in Fig. 6. The apparent variations in the surface structure in our constant-current mode STM images, even over a single terrace, can be correlated with the tip-sample distance. Assuming, to a first approximation, that our STM z scale can be correlated with the physical tip-sample distance given the homogeneity of the surface states observed, over the darker areas (tip closer to the sample) the classical 1×1 predominates [Fig. 6(b)] whereas in the relatively brighter areas (tip farther from sample) the 2×1 dihydride structure [Fig. 6(a)] is observed.

Thus, the observed “ 2×1 ” dihydride structures in the STM images could be due to the dihydride groups being canted or perhaps “domain-boundary” dihydrides alternating with canted dihydrides³⁵ [see Fig. 1(f)]. Such a structure may be polarizable in the vicinity of the STM (or NC-AFM) tip leading to variations in the images according to the sample-tip distance which would explain the images observed. The fact that these dihydride structures are indeed polarizable, however, could also be due to hydrogen bound to the first subsurface layers following the attack at weakened Si-Si backbonds thus conferring a greater polarizability to the surface dihydride structures. This would explain both the symmetrical 1×1 images [Fig. 6(b)] as well as their changes with different tip-sample distances in both STM [Fig. 6(a)] and in NC-AFM.³⁶ Moreover, the different polarizabilities of alternating dihydride rows observed in the STM images may help provide a key to explaining how the subsurface bonds would be affected. The idea of hydrogen being bound to subsurface silicon in some kind of well-defined manner would also explain the TPD results where a clear distinct

desorption peak, referred to as α , is observed at $\approx 700^\circ\text{C}$.

Summarizing, the STM results confirm not only the conclusions drawn from the interpretation of the other analytical data (uniform surface, presumably dihydride) but also the extent (around 90%) of the dihydride over all areas of the surface examined as well as its stability both during transport and when subjected to temperatures of up to 200°C in UHV.

That the surface has dihydride terminations is moreover supported by TPD. The TPD spectrum is usually considered able to provide information on hydrogen terminations through the relative intensities of desorption peaks β_2 at $\approx 300^\circ\text{C}$ (attributed to H_2 elimination from vicinal dihydride silicon atoms) and β_1 at $\approx 510^\circ\text{C}$ (attributed to H_2 elimination from monohydride dimers).¹⁰ The very fact that the spectra of samples (b₁) and (c) have β_2 and β_1 peaks with approximately the same intensity is thus consistent with the fact that the surface is entirely covered by SiH_2 terminations.

The spectral region at $T > 600^\circ\text{C}$ is of interest too. In this region reference sample (a) gives evidence for an emission shoulder. This emission may be attributed to H_2 elimination from geminal dihydrogen terminations in residual unreacted SiH_2 groups, vicinal monohydrogen terminations not belonging to the same $(\text{SiH})_2$ dimer, etc. (Evidence for such a shoulder for (100) and (111) HF_{aq} -etched surfaces is also given in Ref. 37.) The TPD spectrum of sample (c), annealed at 1100°C , shows instead clear-cut evidence for an emission peak (α hydrogen) at $\approx 650\text{--}700^\circ\text{C}$. Sample (b₁), annealed at 850°C , has in the considered region an intermediate spectrum between those of (a) and (c). Emission peaks at $650\text{--}700^\circ\text{C}$ have been observed for *rough* surfaces exposed to atomic hydrogen at a temperature between 420 and 530 K (and attributed to the desorption of a reactive form of subsurface hydrogen)³⁸ or for hydrogen-implanted silicon (and attributed to the desorption of H_2 molecules embedded in cavities or desorbed from the their inner walls).³⁹ Consistently with these observations, we hypothesize that *α hydrogen is actually due to hydrogen trapped in vacancylike defects (vacancy clusters or cavities) injected into the subsurface region during the flattening transition.*

If this interpretation is correct, the XPS data at different takeoff angles should give evidence for it. Actually, following our previous analysis,²⁰ the entire family of XPS spectra may be explained assuming the presence of three features in addition to that of elemental silicon $\text{Si}^{(0)}$:

$\text{Si}^{(\oplus)}$, with $\Delta E_{\oplus/0} = (0.27 \pm 0.01)$ eV

$\text{Si}^{(\oplus\oplus)}$, with $\Delta E_{\oplus\oplus/0} = (0.56 \pm 0.05)$ eV

$\text{Si}^{(\ominus)}$, with $\Delta E_{\ominus/0} \approx -(0.24 \mp 0.02)$ eV,

where $\Delta E_{x/0}$ denotes the chemical shift of feature $\text{Si}^{(x)}$ ($x = \oplus, \oplus\oplus, \ominus$) with respect to $\text{Si}^{(0)}$. The sign and values of $\Delta E_{\oplus/0}$ and $\Delta E_{\oplus\oplus/0}$ suggest that they may be reasonably attributed to silicon hydrides, not better specified at this level of investigation. The sign and value of $\Delta E_{\ominus/0}$ might indicate clean silicon dimers⁵ as responsible for this feature; however, if not due to clean silicon dimers at the inner surface of cavities, the persistence of this signal after prolonged exposure to air suggests that it be considered as a minor correction to the assumed line shape [70% of Gaussian character, with a tail length of 6.5 and tail scale of 0.6% (Ref. 40)] of

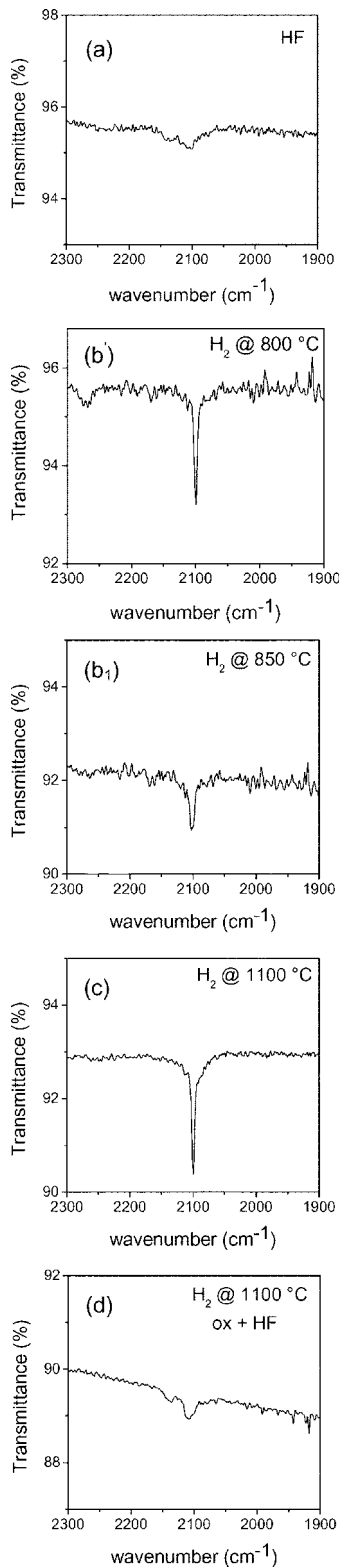


FIG. 7. Comparison of the infrared absorption spectra from (100)-Si surfaces resulting after (a) etching in HF_{aq} an as received slice; (b') heating in H_2 at 800°C for 20 min a HF_{aq} -etched surface; (b₁) heating in H_2 at 850°C for 1 min an HF_{aq} -etched surface; (c) heating in H_2 at 1100°C for 3 min a HF_{aq} -etched surface; and (d) oxidizing the surface treated in H_2 at 1100°C with a piranha solution and removing the oxide so formed with HF_{aq} .

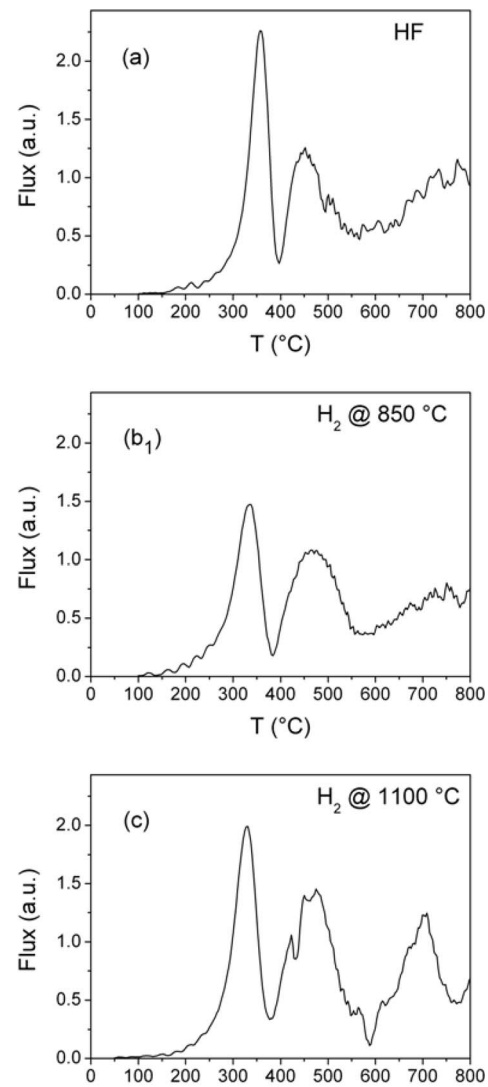


FIG. 8. TPD spectra from a (100)-Si surface resulting after (a) etching in HF_{aq} an as-received slice; (b₁) treating it in H_2 at 850°C for 1 min; and (c) treating the HF_{aq} -etched slice in H_2 at 1100°C for 3 min.

elemental silicon. The data did not allow us to assign the space region responsible for all these features: only $\text{Si}^{(\ominus)}$ was unambiguously found to have a superficial nature (hence its attribution), the combination of features $\text{Si}^{(\oplus)}$ and $\text{Si}^{(\oplus\oplus)}$ was found to originate not only from the surface but also from a region extending into the bulk for several electron mean free paths, at least.¹⁶ This information is extracted from the log-log plot of $\ln(1+f_x/f_0)$ versus $(\sin \theta)^{-1}$ (with f_x the normalized intensity of $\text{Si}^{(x)}$) in Fig. 10, remembering that a slope of 1 would be evidence for a purely superficial distribution, while a slope of 0 would be evidence for a uniform in-depth distribution.

Assuming the correctness of the above interpretation, however, two questions remain unanswered:

(i) Why the exposure to H_2 at $T < 800^\circ\text{C}$ at lower pressure (though only by a factor of 1/4) than that considered in this work followed by cooling in H_2 to room temperature results in monohydride, 2×1 (100) silicon surfaces.^{11,12}

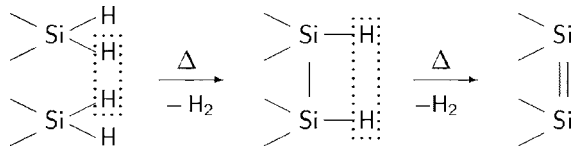
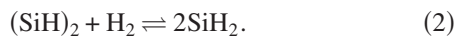
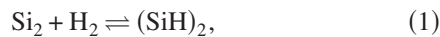


FIG. 9. Consecutive reactions supposedly responsible for hydrogen desorption from homogeneous and flat hydrogen-terminated (100) Si.

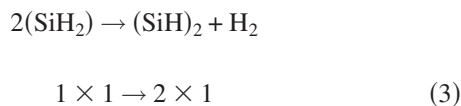
(ii) How it is possible that dihydrogen terminations survive in the quenching phase, taking into account that they are destroyed on heating at 300 °C for a few tens of seconds,⁴¹ as shown in Fig. 8.

To remove the first anomaly, we assume that clean Si₂ dimers transform first into hydrogen-terminated dimers (SiH)₂ and then into dihydrogen-terminated monomers SiH₂ via oxidative addition of H₂



We then observe that the difference between the dihydrogen terminations reported here, and monohydrogen terminations (reported for instance in Refs. 11 and 12) can hardly be understood in terms of a shift in equilibrium (2) toward the right-hand side, due to the relatively modest difference in pressure. Rather, both the 1×1 dihydride surface and the 2×1 monohydride surface may be explained in terms of quenching procedures: Presumably relatively slow in the arrangement of Ref. 11 (because the sample is brought into the *vacuum* system for RHEED analysis) and certainly slow (≈ -1 °C s⁻¹) in the experiment of Ref. 12; very fast (expectedly of the order of -10^2 °C s⁻¹) in the present case, because forced by the strong N₂ flux in the transfer chamber.

The process



is associated with overcoming a lower energy barrier but requires a much higher activation entropy than that of the emission of the β_2 peak observed in TPD (thus involving several correlated moves). It may therefore be manifested only for treatments involving a low cooling rate at temperatures around 500 °C and not otherwise. In this way we assume that in the experiments of Aoyama *et al.*¹¹ and Kumagai *et al.*¹² the treatments at moderate temperature in the furnace actually produced 1×1 dihydrogen terminations but the prolonged exposure at ≈ 500 °C activated reaction (3).

The flattening and homogenization of the surface after the heat treatment (shown in Figs. 3 and 7) is thus the final result of a complex process involving: (i) the injection into the subsurface region of hydrogen-decorated vacancies; (ii) their agglomeration in clusters and eventually their reorganization as cavities; (iii) H₂ emission into the cavity from its inner walls; (iv) the evaporation of such molecules into the silicon crystal; and (v) the out-diffusion of dissolved H₂ molecules.

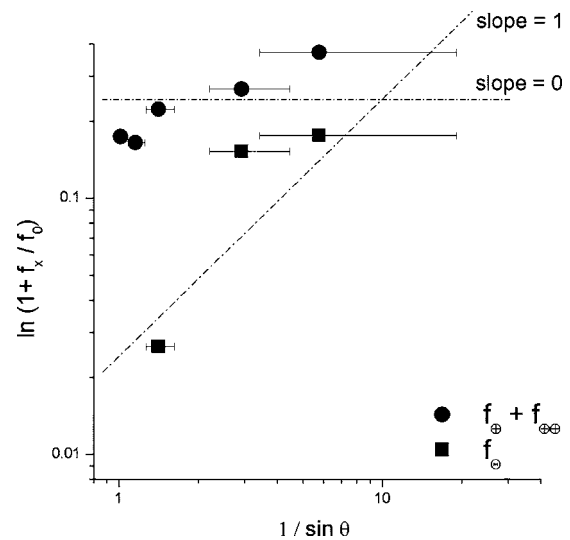


FIG. 10. Log-log plots of $\ln(1+f_x/f_0)$ versus $(\sin \theta)^{-1}$.

This picture suggests an interpretation of the presence of the small holes (or pits) observed by STM and not yet interpreted: they might be vacancy agglomerates not completely embedded in the subsurface region.⁴² In this scheme the dihydride surface prepared at high temperature in H₂ atmosphere is continuously restored to SiH₂ by the reaction of out-diffusing H_{2(sol)} with superficial SiH terminations. This process is facilitated by the fact that H_{2(sol)} is more reactive than H₂ in the gas phase, H_{2(g)}, as confirmed by its lower binding energy [3.8 eV for H_{2(sol)} (Ref. 43) versus 4.6 eV for H_{2(g)}]. This interpretation is sustained by the observation of a TPD emission peak 700 °C (α peak) attributed to hydrogen buried beneath the silicon surface.

The presence of buried hydrogen may also explain the prevalence, increasing with T , of SiH₂ over (SiH)₂ terminations. At a first glance this result seems paradoxical, because the vicinity of the internal energies of products and reactants⁴⁴ in equilibrium (2) would produce an (SiH)₂/SiH₂ relative abundance *decreasing* with T . If not due to kinetic factors, this behavior can be understood by considering the presence of buried hydrogen even in the quenching phase, when the H_{2(g)} external pressure is null: Assuming that H_{2(sol)} is distributed in a region of, say, 10 nm, it should produce an equivalent internal pressure of the order of 10⁶ Pa.

V. CONCLUSIONS

A rapid thermal process of (100) silicon (based on heating to above 850 °C) in H₂, cooling to 670–700 °C in the same environment, and quenching to room temperature in N₂) has been considered. Data based on AFM, STM, ATR-IRAS, TPD, RHEED, and XPS have been interpreted assuming that the preparation results in nearly flat, terraced, dihydrogen terminated, 1×1 (100) silicon surfaces protected by a subsurface layer of buried hydrogen.

The analytical data and their interpretation show the intimate relationships between the morphology and the chemistry of these surfaces.

*Corresponding author. Electronic address:

gianfranco.cerofolini@st.com

- ¹H. Herrmann, H. Herzer, and E. Sirtl, *Festkoerperprobleme* **15**, 279 (1975).
- ²W. Lin and H. Huff, in *Handbook of Semiconductor Manufacturing Technology*, edited by Y. Nishi and R. Doering (M. Dekker, New York, NY, 2000), p. 35.
- ³G. F. Cerofolini and L. Meda, *Appl. Surf. Sci.* **89**, 351 (1995).
- ⁴G. F. Cerofolini, *Appl. Surf. Sci.* **133**, 108 (1998).
- ⁵F. J. Himpsel, F. R. McFeely, A. Taleb-Ibrahimi, J. A. Yarmoff, and G. Hollinger, *Phys. Rev. B* **38**, 6084 (1988).
- ⁶M. Morita, T. Ohmi, E. Hasegawa, M. Kawakami, and M. Ohwada, *J. Appl. Phys.* **68**, 1272 (1990).
- ⁷G. F. Cerofolini, G. La Bruna, and L. Meda, *Appl. Surf. Sci.* **93**, 255 (1996).
- ⁸M. Terashi, J. Kuge, M. Shinohara, D. Shoji, and M. Niwano, *Appl. Surf. Sci.* **130-132**, 260 (1998).
- ⁹Y. Morita and H. Tokumoto, *Appl. Phys. Lett.* **67**, 2654 (1995).
- ¹⁰H. N. Waltenburg and J. T. Yates, *Chem. Rev. (Washington, D.C.)* **95**, 1589 (1995).
- ¹¹T. Aoyama, K. Goto, T. Yamazaki, and T. Ito, *J. Vac. Sci. Technol. A* **14**, 2909 (1996).
- ¹²Y. Kumagai, K. Namba, T. Komeda, and Y. Nishioka, *J. Vac. Sci. Technol. A* **16**, 1775 (1998).
- ¹³F. M. Zimmermann and X. Pan, *Phys. Rev. Lett.* **85**, 618 (2000).
- ¹⁴E. J. Buehler and J. J. Boland, *Science* **290**, 506 (2000).
- ¹⁵G. F. Cerofolini, C. Galati, S. Lorenti, L. Renna, O. Viscuso, C. Bongiorno, V. Raineri, C. Spinella, G. G. Condorelli, I. L. Fragalà, and A. Terrasi, *Appl. Phys. A: Mater. Sci. Process.* **77**, 403 (2003).
- ¹⁶G. F. Cerofolini, C. Galati, and L. Renna, *Surf. Interface Anal.* **35**, 968 (2003).
- ¹⁷G. F. Cerofolini, C. Galati, S. Reina, L. Renna, F. Giannazzo, and V. Raineri, *Surf. Interface Anal.* **37**, 71 (2004).
- ¹⁸G. F. Cerofolini, C. Galati, G. Giorgi, A. Motta, S. Reina, L. Renna, and A. Terrasi, *Appl. Phys. A: Mater. Sci. Process.* **81**, 745 (2005).
- ¹⁹G. F. Cerofolini, M. Camalleri, C. Galati, S. Lorenti, L. Renna, O. Viscuso, G. G. Condorelli, and I. L. Fragalà, *Appl. Phys. Lett.* **79**, 2378 (2001).
- ²⁰G. F. Cerofolini, C. Galati, and L. Renna, *Surf. Interface Anal.* **34**, 583 (2002).
- ²¹H. J. W. Zandvliet, *Rev. Mod. Phys.* **72**, 593 (2000).
- ²²K. Arima, K. Endo, T. Kataoka, Y. Oshikane, H. Inoue, and Y. Mori, *Appl. Phys. Lett.* **76**, 463 (2000).
- ²³K. Endo, K. Arima, K. Hirose, T. Kataoka, and Y. Mori, *J. Appl. Phys.* **91**, 4065 (2002).
- ²⁴V. Palermo and D. Jones, *Mater. Sci. Semicond. Process.* **4**, 437 (2001).
- ²⁵J. J. Boland, *Adv. Phys.* **42**, 129 (1993).
- ²⁶E. J. Buehler and J. J. Boland, *Surf. Sci.* **425**, L363 (1999).
- ²⁷Actually this conclusion is essentially based on the analysis of the Si $2p$ spectra of Fig. 2. It is however noted that in practically all cases we detected both adventitious carbon (≈ 0.2 monolayer, attributed to physisorbed organic contaminants) and an amount of about 1 monolayer of oxygen, which could not be attributed to oxidized carbon. The bonding state of such an oxygen has not been clarified yet.
- ²⁸F. S. Tautz and J. A. Schaefer, *J. Appl. Phys.* **84**, 6636 (1998).
- ²⁹M. K. Weldon, V. E. Marsico, Y. J. Chabal, A. Agarwal, D. J. Eaglesham, J. Sapjeta, W. L. Brown, D. C. Jacobson, Y. Caudano, S. B. Christman, and E. E. Chaban, *J. Vac. Sci. Technol. B* **15**, 1065 (1997).
- ³⁰Y. J. Chabal and K. Raghavachari, *Phys. Rev. Lett.* **54**, 1055 (1985).
- ³¹In fact, the 1×1 (100) SiH_2 surface, obtained by suitable exposure to H of the “perfect” clean 2×1 (100) Si surface, does not restore the original structure at once. Rather upon heating to above 500°C and complete hydrogen desorption, the 2×1 phase appears between silicon clusters and reverts upon further annealing at $570\text{--}690^\circ\text{C}$ to the metastable $c(4 \times 4)$ phase before transforming into the well-ordered 2×1 phase by annealing above 700°C . See K. Kato, T. Ide, T. Nishimori, and T. Ichinokawa, *Surf. Sci.* **207**, 177 (1988); T. Ide and T. Mizutani, *Phys. Rev. B* **45**, 1447 (1992); R. I. G. Uhrberg, J. E. Northrup, D. K. Biegelsen, R. D. Bringans and L.-E. Swartz, *ibid.* **46**, 10251 (1992); Y. Wang, M. Shi, and J. W. Rabalais, *Phys. Rev. B* **48**, 1678 (1993); M. Yoshimura and K. Ueda, *Appl. Surf. Sci.* **121/122**, 179 (1997).
- ³²S.-S. Ferng, C.-T. Lin, K.-M. Yang, D.-S. Lin, and T.-C. Chiang, *Phys. Rev. Lett.* **94**, 196103 (2005).
- ³³J. E. Northrup, *Phys. Rev. B* **44**, R1419 (1991).
- ³⁴K. Tagami and M. Tsukada, *Surf. Sci.* **384**, 308 (1997).
- ³⁵K. Tagami and M. Tsukada, *Surf. Sci.* **400**, 383 (1998).
- ³⁶S. Araragi, A. Yoshimoto, N. Nakata, Y. Sugawara, and S. Morita, *Appl. Surf. Sci.* **188**, 272 (2002).
- ³⁷N. Hirashita, M. Kinoshita, I. Aikawa, and T. Ajioka, in *Semiconductor Silicon 1990*, edited by H. R. Huff, K. G. Barraclough, and J. Chikawa (The Electrochem. Soc., Pennington, NJ, 1990), p. 313.
- ³⁸S. K. Jo, J. H. Kang, X. Yan, J. M. White, J. G. Ekerdt, J. W. Keto, and J. Lee, *Phys. Rev. Lett.* **85**, 2144 (2000).
- ³⁹F. Corni, C. Nobili, R. Tonini, G. Ottaviani, and M. Tonelli, *Appl. Phys. Lett.* **78**, 2870 (2001).
- ⁴⁰Z. H. Lu, M. J. Graham, D. T. Jiang, and K. H. Tan, *Appl. Phys. Lett.* **63**, 2941 (1993).
- ⁴¹As mentioned in the introduction, dihydrogen terminated 1×1 (100) Si may also be prepared via exposure to atomic hydrogen H, however *at a lower temperature* (300 K) *than that of the emission of the β_2 peak*.
- ⁴²Other interpretations are however possible: For instance, the bright features are reminiscent of the “bright bumps” previously observed and attributed to $-\text{SiH}_3$ terminations [see, for instance, X. R. Qin and P. R. Norton, *Phys. Rev. B* **53**, 11100 (1996)], and dark-to-bright changes over time could be explained by the existence at the surface of “bright” $-\text{SiH}_3$ species followed by SiH_4 loss leading to etching and “dark” pit formation. This is known to be an important mechanism causing instability of the dihydride surface.
- ⁴³C. G. Van de Walle, *Phys. Rev. B* **49**, 4579 (1994).
- ⁴⁴Taking the following bond dissociation energies, $E_b[\text{H-H}] = 4.5$ eV, $E_b[\text{Si-H}] = 3.5$ eV; $E_b[\text{Si-Si}_{\text{dimer}}] = 2.0$ eV [at (100) 2×1 SiH], the products of reaction (2) are more stable than the reactants by only 0.5 eV. The datum for $E_b[\text{Si-Si}_{\text{dimer}}]$ is taken from A. Ramstadt, G. Brocks, and P. J. Kelly, *Phys. Rev. B* **51**, 14504 (1995).